Bisphenolic Compounds That Enhance Cell Cation Transport Are Found in Commercial Phenol Red

Philip R. Kym,[†] Kim L. Hummert,[†] Anna G. Nilsson,[†] Martin Lubin,[‡] and John A. Katzenellenbogen*[,†]

Department of Chemistry, University of Illinois, Urbana, Illinois 61801, and Department of Microbiology, Dartmouth Medical School, Hanover, New Hampshire 03755

Received April 22, 1996[⊗]

We have isolated two bisphenolic compounds (**4** and **5**) that have a marked effect on K^+ and Na^+ concentrations in human cells from commercial preparations of the pH indicator dye phenol red (phenolsulfonphthalein). We used a bioassay to identify active chromatographic fractions from the lipophilic impurities present in phenol red, and we determined the structure of two active components (**4** and **5**) by ^1H and ^{13}C NMR and mass spectrometry. When added to human fibroblasts in serum-free medium, the bisphenol fluorene derivative 9,9-bis(4′-hydroxyphenyl)-3-hydroxyfluorene (**5**) produced a rapid loss of K^+ and a gain of Na^+, at low concentrations, with an EC_{50} between 30 and 60 ng/mL (80−160 nM). The 2- and 4-hydroxy isomers of the fluorene **5** (i.e., compounds **6** and **7**), prepared by synthesis, had similar activity, although compound **6** was somewhat less potent. The bisphenol xanthene derivative 9,9-bis(4′-hydroxyphenyl)xanthene (**4**) elicited a similar biological response but was less potent than **5**−**7**; it also had a strong effect on cell adhesion, causing release of cells from the plastic substrate at concentrations as low as 2−5 μg/mL (5.5−14 μM). The structures of xanthene (**4**) and fluorene (**5**) bisphenols have been confirmed by synthesis from xanthone and hydroxyfluorenone, respectively, by Friedel-Crafts alkylation with phenol. In the latter case, the desired 3-hydroxyfluorene isomer was formed *in situ* by rearrangement of the 1-hydroxy isomer.

Introduction

Phenol red (phenolsulfonphthalein, **1**) has been used for almost a century to evaluate many biological processes, including measurement of renal tubular function,[1] estimation of kidney blood flow,[2] and measurement of lipid and hydrogen peroxide formation.[3] Its most far-reaching and common use, however, is as a pH indicator in tissue culture media. Commercially, phenol red is prepared in one step by the acid-catalyzed Friedel−Crafts reaction of phenol with 2-sulfobenzoic acid, 2-sulfobenzoic acid cyclic anhydride, or saccharin at elevated temperatures.[4] Excess phenol functions as solvent, and yields are good. Most commercial preparations of phenol red are sold at a purity of 90% or 95% "dye content", with the remaining 5−10% of material consisting of lipophilic impurities.

Some time ago, commercial preparations of phenol red were shown to have weak estrogenic activity in several estrogen-dependent human breast cancer-derived cell lines (MCF-7,[5] T47D,[6] ZR-75-1[7]). Although the estrogenic activity observed with phenol red preparations was initially attributed to the phenolsulfonphthalein dye itself,[5−7] later studies showed it to be due to a lipophilic impurity present in the phenol red preparation.[8] This impurity was isolated and characterized as the phenyl sulfonate ester of the reduced form of phenol red (**2**) which is found together with its oxidized congener (**3**) (Figure 1).[9] Phenol red preparations have also been identified as the source of cytotoxicity in MCF-7 breast cancer cells under alkaline (pH > 7.4)

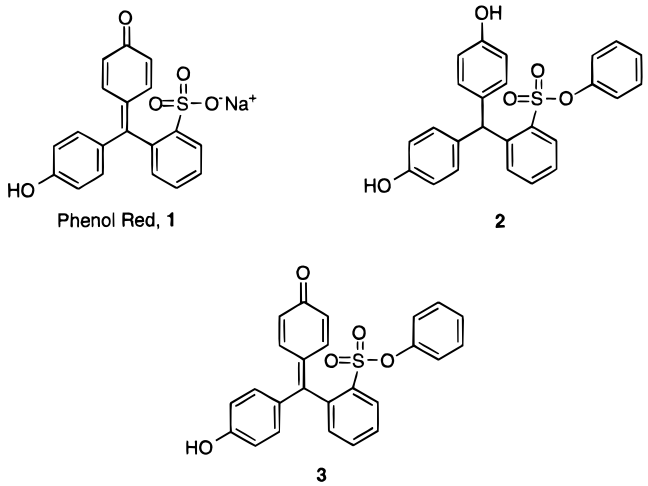

Figure 1. Structures of phenol red (**1**), estrogenic lipophilic impurity **2**, and oxidized estrogenic impurity **3**.

conditions,[10] as an inhibitor of a thromboxane A_2/prostaglandin H_2 receptor agonist,[11] and as an inhibitor of renal epithelial cell growth.[12]

Recently, one of us (M. Lubin) found that impurities in samples of several commercial preparations of phenol red caused rapid loss of cell K^+ and gain of Na^+ (with a reversal of the normally high K^+/Na^+ ratio) in human MCF-7, EJ bladder carcinoma, and fibroblast (HF) cells, when cells were incubated in serum-free medium.[13] This action on ion transport was effectively inhibited by albumin or serum, which presumably absorbed most of the impurities. Moreover, an ether extract of phenol red was active in the bioassay, but the residual extracted phenol red was not. The ion channel blockers quinine and verapamil partially inhibited the action of the impurities. Interestingly, the effects observed with phenol red in human MCF-7, EJ, and HF cells were not apparent in the rodent NIH-3T3 or CHO-K1 cell lines.

* Address correspondence to: Prof. John Katzenellenbogen, Department of Chemistry, University of Illinois, Box 37 Roger Adams Laboratory, 600 S. Mathews Ave., Urbana, IL 61801. E-mail: jkatzene@uiuc.edu.
[†] University of Illinois.
[‡] Dartmouth Medical School.
[⊗] Abstract published in *Advance ACS Abstracts,* November 15, 1996.

S0022-2623(96)00300-7 CCC: $12.00 © 1996 American Chemical Society

Hopp and Bunker have also recently reported that lipophilic impurities in phenol red cause a reversal of cell K^+/Na^+ ratio in human fibroblasts and COS-7 and Hs68 cell lines.[14] A change in the intracellular K^+ and Na^+ of the magnitude observed by Lubin, and by Hopp and Bunker, would be expected to have an effect on multiple cellular functions. Furthermore, the observation that crude phenol red preparations were active suggested that the responsible components may be very potent, since it is likely that these components make up less than 1% of the total material present.

In this report, we describe the isolation and structure determination of compounds in the lipophilic extract of commercial phenol red that display ion transport activity or toxicity. We used reversed-phase HPLC to fractionate the impurities, and guided by a bioassay, we were able to identify those fractions with maximum activity and isolate two active substances. We determined their structures by spectroscopy, confirmed them by synthesis, and tested them, and certain analogs, in cell culture assays.

Results and Discussion

Isolation and Identification of Components That Cause Loss of Cell K^+. Our strategy for identifying components of phenol red preparations that possess biological activity involved four steps: (1) solvent partitioning of the lipophilic impurities of phenol red, (2) reversed-phase HPLC analysis of the lipophilic impurities, (3) systematic bioassay of crude fractions to identify active components, and (4) final purification and identification of active components.

Extraction of a 5.42 g portion of phenol red monosodium salt (Aldrich) with diethyl ether (3 × 50 mL) provided 0.127 g (2.4%) of a reddish brown oil. Analytical reversed-phase HPLC of this material revealed the presence of about 20 different lipophilic components; most of the mass (about 90%) was present in six major peaks (Figure 2, panel A). The eluent containing the major lipophilic impurity (t_R = 11 min) was deep red; this component had previously been identified as the oxidized estrogenic impurity **3**.[9] The estrogenic impurity **2** had previously been identified as the minor peak at t_R = 13 min.[8] The identity of these peaks was confirmed by coinjection of authentic samples.

We initially tested the effect of the crude lipophilic impurities on intracellular K^+ and Na^+ in HF cells, using the procedure previously described.[13] We found that incubation of the crude material from the ether extract changed the intracellular ratio of K^+/Na^+ from 7.4 to 0.68 (Table 1) (typical ratios observed in healthy cells range from about 3.5 to 10).[13] Encouraged by this preliminary result, we proceeded with preparative reversed-phase HPLC fractionation of the crude ether extract. Since the resolution of the preparative scale separation was poorer than the analytical scale separation (cf., Figures 2 and 3), we collected only 10 fractions (fractions I−X, Figure 3) and assayed them for their effect on the K^+ and Na^+ content of HF cells.

We found that two of the collected fractions possessed significant biological activity (Table 1). Fraction II caused a dramatic effect on the K^+/Na^+ ratio, dropping it to 0.30, almost completely reversing the value typically observed in healthy cells. Fractions III and IV showed a weak effect, possibly attributable to small amounts of the potent component from fraction II that

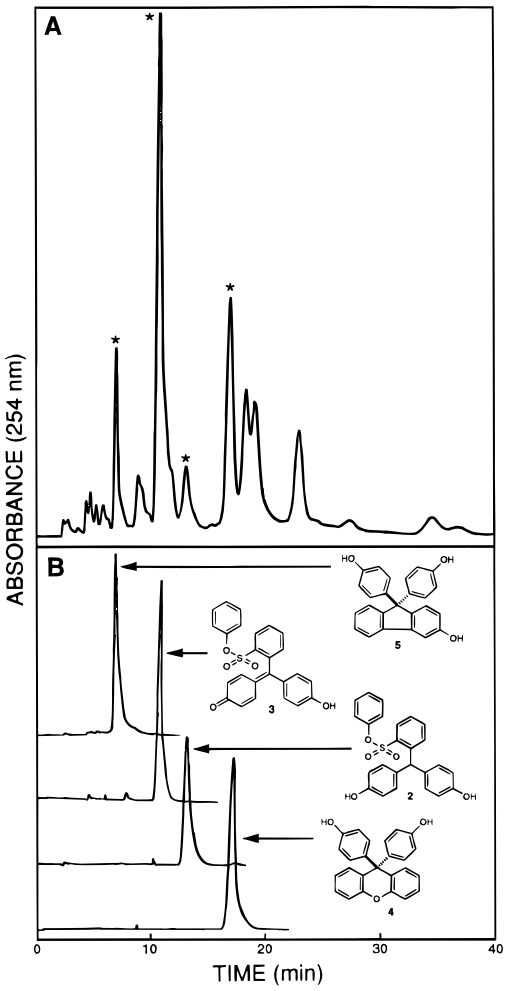

Figure 2. Panel A: Reversed-phase analytical HPLC of the ether extract of phenol red sodium salt (C-18 silica gel column; 1 mL/min eluting with isocratic 50:50 water:acetonitrile; UV absorbance monitored at 254 nm). Panel B: Alignment of characterized, pure components from the ether extract of phenol red with the HPLC trace from the crude lipophilic impurities; the starred peaks in panel A correspond to the pure components in panel B. HPLC conditions were identical with those described for panel A.

may have been present in these tail fractions. Fraction VII also demonstrated weak activity in the bioassay, as the observed ratio of K^+/Na^+ was 1.7. The more pronounced effect of fraction VII, however, was its apparent cytotoxicity. After 1 h of incubation with fraction VII, most of the fibroblasts were partly retracted, and a few of the cells had detached themselves from the culture dish. Since the effect of fraction VII on ion content was less than that of fraction II, its toxic effect on adhesion is probably not due to its effect on ion distribution.

Reevaluation of fraction VII by analytical reversed-phase HPLC revealed only two components, present in a ratio of about 9:1. We were able to isolate 4.4 mg of the major component in pure form by silica gel flash chromatography (50% hexanes/EtOAc). Injection of fraction II onto the analytical column also revealed only one major component. We repeated the ether extraction on 25 g of the same lot of phenol red (Aldrich) and isolated 0.418 g of lipophilic impurities. Initial purification of the ether extract was accomplished by normal phase silica gel chromatography (gradient elution from 80% hexanes in EtOAc to 100% EtOAc). A portion of the fraction that contained the components of fraction

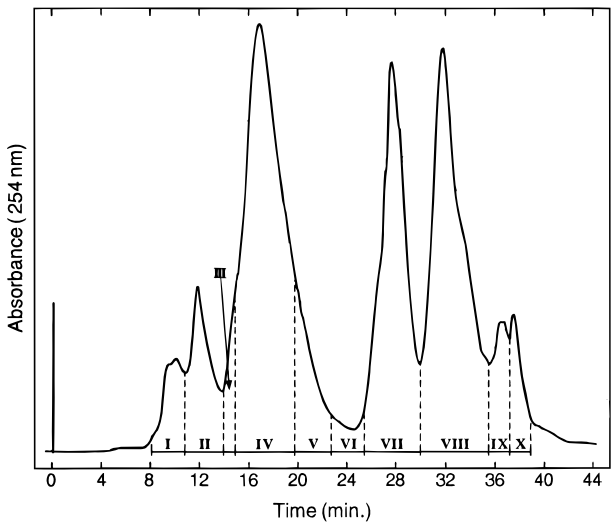

Figure 3. Crude partitioning of the lipophilic impurities of phenol red by preparative reversed-phase HPLC (C-18 silica gel column; 3 mL/min with water:acetonitrile gradient starting from 50:50 (first 20 min), increasing to 20:80 over 10 min, and maintaining 20:80 for 20 min; UV absorbance monitored at 254 nm).

Table 1. Effect of Crude HPLC Fractions from Lipophilic Impurities in Phenol Red on Ion Content of HF Cells[a]

additive	K^+	Na^+	K^+/Na^+
control	35	4.7	7.4
purified phenol red	34	4.4	7.7
crude impurities	17	25	0.68
HPLC Fr I	35	4.9	7.1
II	10	33	0.30
III	28	14	2.0
IV	30	10	3.0
V	38	5.0	7.6
VII	27	16	1.7
VIII	35	4.4	8.0
IX	36	4.1	8.8
X	35	5.3	6.6

[a] Each of the nine fractions displayed in Figure 3 was dried, taken up in equal volumes of ethanol, and then added to DMEM without phenol red or serum and applied to cell cultures. Final solvent concentration was 0.1%. Purified phenol red was at 15 μg/mL, and crude impurities were at 2.7 μg/mL. Final concentrations of each HPLC fraction, in μg/mL: I, 4.5; II, 6.3; III, 7.5; IV, 10.1; V, 4.2; VII, 24.3; VIII, 3.5; IX, 0.4; X, 0.4. After 45 min at 37 °C in CO_2/air, cells were processed for analysis. Values shown are $10^8 \times$ mol of K^+ or Na^+ per dish, assayed as described previously.[13]

II was subjected to preparative reversed-phase HPLC (50% CH_3CN:H_2O, isocratic). From these chromatographic runs, 2.4 mg of the major component of fraction II was isolated.

The pure major components of fractions II and VII were reevaluated by bioassay for K^+ and Na^+. We found that these components produced a more pronounced effect on K^+/Na^+ ratios than had been previously observed for the crude fractions; therefore, we were confident that they were the principal source of the biological activity. The traces from pure samples of fractions II and VII, as well as pure samples of the estrogenic compound **2** and its oxidized form **3**, are aligned with the peaks to which they correspond in the analytical reversed-phase HPLC trace of the crude lipophilic impurities of phenol red (Figure 2).

Structure Elucidation of the Major Component in Fraction VII. Electron-impact (EI, 70 eV) and field-desorption (17 μA) mass spectrometry of the purified material from fraction VII gave an intense molecular ion at m/z 366, which at high resolution gave a mass at 366.1256, calcd 366.1256, indicating a composition of $C_{25}H_{18}O_3$. The most prominent fragment was 273 ($M^+ - 93$), indicative of loss of a phenol group.

The 500 MHz J-correlated 2D ^1H NMR spectrum established the presence of a 1,4-disubstituted aromatic four-spin (AA′XX′) system (two doublets at δ 6.73 and 6.58, $J = 8.8$ Hz, equivalent to four protons each). The remaining eight protons were nested in a 1,2-disubstituted aromatic four-spin (ABCD) system, indicated by the two sets of doublet of doublet of doublets (δ 7.21, 6.99) and two sets of doublet of doublets (δ 7.07, 6.93), each set equivalent to four protons. The only other signal was a singlet (equivalent to two protons) at δ 8.22.

The simplicity of the ^1H NMR spectrum (a 1,4-disubstituted four-spin system, a 1,2-disubstituted four-spin system, and a singlet), coupled with the elemental composition ($C_{18}H_{25}O_3$) available from high-resolution mass spectrometry, suggested that this compound possesses a plane of symmetry. This symmetry was further supported by the ^{13}C NMR spectrum, which revealed the presence of only 11 unique carbon centers.

The $^1H-^{13}C$ chemical shift correlation spectrum showed the presence of five quaternary carbons and six carbon centers that correlated with proton resonances. The five quaternary carbons are assigned following literature precedent[15] and comparison with the ^{13}C NMR spectrum for **5**, the two hydroxy-substituted $^{13}C_{4'}$ carbons being the most downfield at δ 156.2 followed by the oxygen-substituted C_{4a} carbons in the xanthene ring system at δ 152.6, the $C_{1'}$ carbons that are *para* to hydroxyl substitution at δ 136.7, the remaining two quaternary C_{1a} carbons of the xanthene system at δ 131.3, and finally the only aliphatic carbon (δ 53.0, C_9) at the tetrahedral center of the molecule.

The combination of the J-correlated 2D ^1H NMR spectrum and the $^1H-^{13}C$-correlated spectrum enabled us to make definitive assignments for the remaining protons and carbons. The $C_{3'}$ carbons in the 1,4-disubstituted aromatic ring systems are the most upfield aromatic resonances at δ 114.3, and the protons attached to these carbons ($H_{3'}$, δ 6.58, *ortho* to the hydroxyl) are the most upfield-shifted proton signals. These protons are coupled to the protons *meta* to the hydroxyl groups ($H_{2'}$, δ 6.73), which are attached to the $C_{2'}$ carbons at δ 130.9. In the 1,2-disubstituted aromatic ring system, the most upfield doublet is assigned as protons H_1, δ 6.93, which are attached to the C_1 carbons (δ 130.1). These protons are most strongly correlated with the doublet of doublets at δ 6.99 (H_2), which are attached to the C_2 carbons (δ 122.5). These protons are coupled to the most downfield protons in the 1,2-disubstituted system (H_3, δ 7.21, *meta* to the oxygen substitution), which are correlated with the C_3 carbons (δ 127.4). The final correlation in this four-spin system is between H_3 (δ 7.21) and H_4 (δ 7.07); the H_4 protons are correlated with the C_4 carbons (δ 116.0).

The corroboration of NMR spectroscopy and mass spectrometry led us to assign the structure of the major component of fraction VII as 9,9-bis(4′-hydroxyphenyl)-xanthene (**4**). The final proof of this structure was provided by the synthesis of **4** from xanthone and phenol (*vide infra*).

Structure Elucidation of the Major Component of Fraction II. Electron-impact (70 eV) and field-

desorption (17 μA) mass spectrometry of the purified material from fraction II gave an intense molecular ion at m/z 366, which at high resolution gave a mass at 366.1254, calcd 366.1256, indicating a composition of $C_{25}H_{18}O_3$. This material was identical in mass and composition with the previously identified fraction VII. Prominent fragments included m/z 348 ($M^+ - 18$) and 273 ($M^+ - 93$), indicating the possible loss of a hydroxyl group and a phenol group, respectively.

The 500 MHz J-correlated 2D ^{1}H NMR spectrum established the presence of a 1,4-disubstituted aromatic four-spin (AA′XX′) system (two doublets at δ 6.95 and 6.53, $J = 8.7$ Hz, four protons each). One 1,2-disubstituted aromatic four-spin (ABCD) system equivalent to four protons is indicated by the two sets of doublets (δ 7.65, 7.31) and the two sets of doublet of doublets (δ 7.24, 7.16). The only remaining correlated spin system is characteristic of a 1,2,4-trisubstituted aromatic spin system indicated by two doublets (δ 7.12, 7.10) and a doublet of doublets (δ 6.62). The two singlets at δ 8.28 and 8.06 correspond to the hydroxyl protons OH_3 and $OH_{4'}$, respectively.

The ^{1}H−^{13}C chemical shift correlation spectrum showed the presence of eight quaternary carbons and nine carbon centers correlated with proton resonances. The quaternary carbons were tentatively assigned following literature precedent[15] and by comparison with the ^{13}C NMR spectrum for **4**. The hydroxyl-substituted $^{13}C_3$ carbon is the most downfield signal at δ 158.1 followed by the two hydroxyl-substituted $C_{4'}$ centers at δ 157.0 and the C_{8a} carbon of the fluorene system at δ 154.0. The other quaternary carbons of the fluorene system (C_{1a}, C_{4a}, and C_{5a}) appear at δ 143.9, 141.9, and 141.0, respectively. The $C_{1'}$ carbons *para* to the hydroxyl substituent in the bisphenol system show up at δ 138.0, while the aliphatic carbon at the tetrahedral center of the molecule appears at δ 64.2.

The combination of the J-correlated 2D ^{1}H NMR spectrum and the ^{1}H−^{13}C correlated spectrum enabled us to make definitive assignments for the remaining protons and carbons. The $H_{3'}$ protons in the 1,4-disubstituted aromatic ring system are the most upfield proton resonances at δ 6.53 and are attached to the $C_{3'}$ carbons (δ 115.2). These protons are coupled to the protons *meta* to the hydroxyl group ($H_{2'}$, δ 6.95), which are attached to the $C_{2'}$ carbons at δ 129.6. In the 1,2-disubstituted aromatic ring system, the most downfield doublet is assigned as proton H_5 (δ 7.65), which is attached to the C_5 carbon (δ 120.3). This proton is *ortho* coupled to the doublet of doublets centered at δ 7.24 (H_6), which correlates to the C_6 carbon (δ 127.4). The doublet at δ 7.31 is assigned to the proton H_8, *ortho* to the quaternary center, which is attached to the C_8 carbon at δ 126.7. This proton is coupled to the proton resonance H_7 (δ 7.16) which is attached to the C_7 carbon at δ 127.7. The protons that are *meta* (H_7) and *para* (H_6) to the quaternary center are also coupled. In the 1,2,4-trisubstituted aromatic ring system, the protons that are *ortho* (H_1, δ 7.10) and *meta* (H_2, δ 6.62) to the quaternary center are *ortho* coupled to each other. The proton that is *meta* to the quaternary center (H_2) is shifted upfield by the resonance-donating effect of the *ortho* hydroxyl group at C_3 of the fluorene ring system. The H_1 proton correlates to the C_1 carbon at δ 127.2 and the H_2 proton is attached to the C_2 carbon at δ 115.4. The H_2 proton is *meta* coupled to the remaining proton (H_4, δ 7.12) which correlates to C_4 at δ 106.9. This proton experiences both the shielding effect of the *ortho* hydroxyl group and the deshielding effect of the edge-on interaction with the second aromatic ring of the fluorene ring system; these opposing electronic influences effectively cancel each other out.

Scheme 1. Synthesis of Bisphenols **4**−**7**

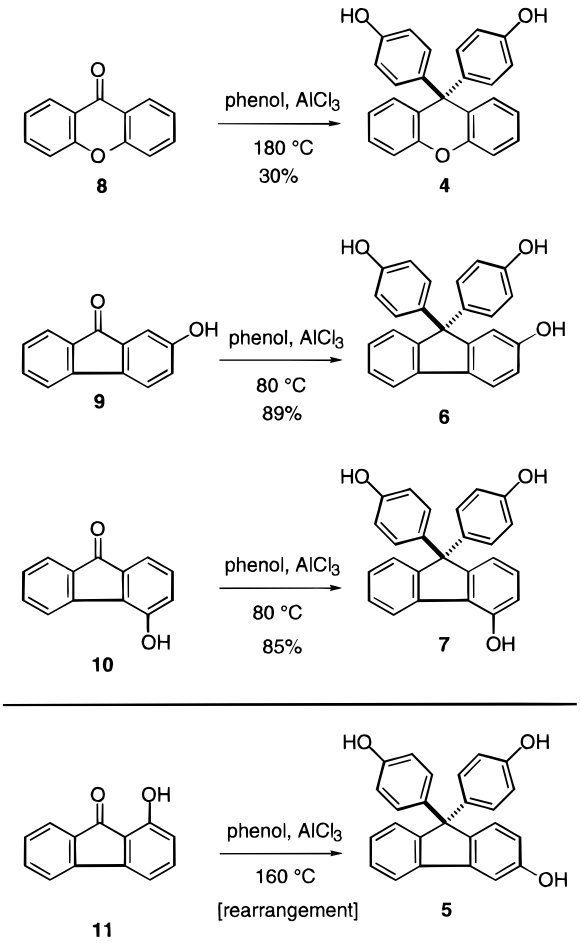

From the combined data from NMR spectroscopy and mass spectrometry, we assign the major component of fraction II from the HPLC separation as 9,9-bis(4′-hydroxyphenyl)-3-hydroxyfluorene (**5**). Final proof of structure for this compound was provided by synthesis from 3-hydroxyfluorenone and phenol (*vide infra*).

Synthesis of Bisphenols 4 and 5. The bisphenol xanthene derivative **4** was available in one step from commercially available phenol and xanthone (**8**) (Scheme 1). Lewis acid-catalyzed phenol addition to the xanthone carbonyl was effected by stirring xanthone (**8**) neat in an excess of phenol with 3 equiv of aluminum chloride. After 4 h at 140 °C, no products that coeluted with the major component of fraction VII isolated by HPLC methods from phenol red had been formed. The reaction mixture was allowed to stir for an additional 12 h at 180 °C, at which point a new spot that coeluted with the major component of fraction VII was observed. The bis-*para*-substituted phenol derivative **4** was the major product isolated (30%) from the reaction mixture. We suspect that the products resulting from alkylation *ortho* to the hydroxyl group are also formed under these forcing conditions. The synthetic material **4** was found to be identical with the material isolated from phenol red, by ^{1}H NMR, mass spectrometry, and HPLC comparisons. Bisphenol **4** has been reported once previously in the literature;[16] it was used as the repeating unit of

novel polycarbonate and polyester polymers with large cross-planar substituents.

From our spectroscopic work, we suspected that the biologically active material in fraction II was a bis(4-substituted phenol) adduct of a hydroxyfluorenone derivative. The *J*-correlated 2D ^{1}H NMR spectrum suggested a 1,2,4-trisubstituted ring system, thus requiring attachment of the hydroxyl group at either the C_2 or C_3 carbons of the fluorene ring system. The position of the hydroxyl group could be unambiguously defined by comparison with authentic bisphenol derivatives of 3-hydroxyfluorenone (**5**) and 2-hydroxyfluorenone (**6**). Our first synthetic target was **6** because 2-hydroxyfluorenone (**9**) is commercially available.

Stirring 2-hydroxyfluorenone (**9**) in excess phenol and aluminum chloride (3 equiv) for 2 h at 80 °C provided the bisphenol **6** in high yield (89%) (Scheme 1). Spectroscopic analysis of this compound (^{1}H and ^{13}C NMR) showed it to be different from the material isolated from phenol red. The most notable difference in the ^{1}H NMR was the presence of two upfield-shifted signals (protons *ortho* to hydroxy substitution) and one downfield-shifted signal (proton in the deshielding region of the second aromatic ring of the fluorenone ring system) in the 1,2,4-trisubstituted aromatic ring system. Although bisphenol **6** was not the same compound as isolated in fraction II from phenol red, it was very similar, and it was evaluated in the bioassay and for relative binding affinity for the estrogen receptor.

In this series, we also prepared the bisphenol derivative (**7**) of 4-hydroxyfluorenone (**10**) (Scheme 1). Stirring commercially available 4-hydroxyfluorenone (**10**) with an excess of phenol and aluminum chloride (3.0 equiv) at 80 °C for 2 h resulted in facile formation of the bisphenol derivative **7** (85%). As expected, this material was also different from the major component in fraction II from phenol red. Our attempt at forming the bisphenol derivative of 1-hydroxyfluorenone (**11**), however, led to a surprising finding (Scheme 1). The starting material, 1-hydroxyfluorenone (**11**), remained unreacted at 80 and 120 °C. Increasing the temperature to 160 °C resulted in formation of a bisphenol product. Isolation of this compound revealed it to be a mixture of two isomers (about 80:20), of which the major isomer was identical with the active component (**5**) in fraction II of phenol red (^{1}H NMR, HPLC). Thus, under the reaction conditions, it appears that the 1-hydroxyfluorene system has rearranged to the 3-hydroxy system.

One can formulate a reasonable mechanism for such a rearrangement: Under forcing reaction conditions, one molecule of phenol attacks the carbonyl group to form the tetrahedral intermediate, which in this C_1−OH system is sterically too crowded to allow attack of the second molecule of phenol. Instead, the C_{1a} carbon is protonated to form a dienone, which fragments at the C_9−C_{1a} bond, allowing for rotation around the C_{4a}−C_{5a} bond of a biphenyl intermediate. Subsequent ring closure by attack of C_9 on the carbon that was originally C_4 results in the monophenol adduct of 3-hydroxyfluorenone. Phenol attack on this less sterically crowded intermediate affords the bisphenol derivative of 3-hydroxyfluorenone.

Confirmation of the structure of the biologically active component isolated in fraction II from reversed-phase HPLC and synthesized by rearrangement from 1-hydroxyfluorenone (**11**) was attained by its synthesis from 3-hydroxyfluorenone (**15**) and phenol (Scheme 2). Synthesis of the 3-hydroxy derivative required 3-hydroxyfluorenone (**15**), which was prepared by Suzuki coupling[17] of the aryl bromide **12** with boronic acid **13**, followed by methanesulfonic acid-catalyzed ring closure and methyl ether deprotection with boron trifluoride−dimethyl sulfide complex (Scheme 2). Aluminum chloride-catalyzed Friedel−Crafts reaction of **15** with phenol provided bisphenol **5** in 81% yield. We have not found any previous reports of bisphenol **5** in the literature.

Scheme 2. Synthesis of 3-Hydroxyfluorenone (**15**)

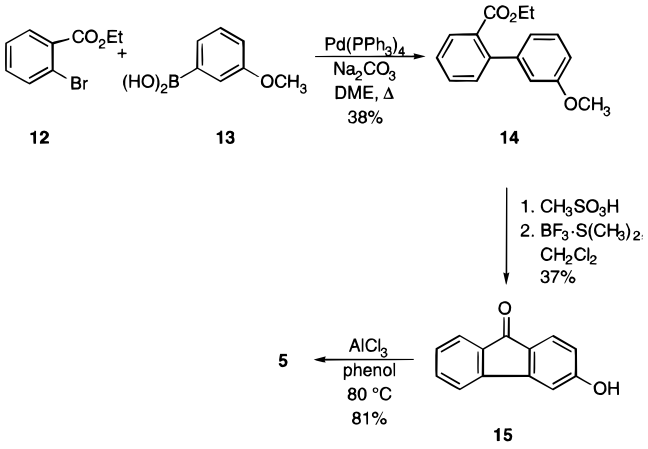

Table 2. Effect of Various Concentrations of Compounds **4**−**7** on Ion Content of HF Cells[a]

expt no.	additive	conctn	K^+	Na^+	K^+/Na^+
I	none	0 ng/mL	30	8.0	3.8
	5	15.6 ng/mL	30	8.0	3.8
	5	31.0 ng/mL	27	12	2.3
	5	62.5 ng/mL	10	29	0.34
	5	125 ng/mL	5.2	38	0.14
	5 + quinine	125 ng/mL	20	22	0.91
	5 + verapamil	125 ng/mL	20	16	1.3
II	none	0 μg/mL	41	10	4.1
	4	2.4 μg/mL	34	19	1.8
	4	4.8 μg/mL	24	27	0.89
III	none	0 μg/mL	43	7.6	5.7
	4	4.8 μg/mL	2.5	29	0.09
	4 + quinine	4.8 μg/mL	27	12	2.3
	4 + verapamil	4.8 μg/mL	37	11	3.4
IV	none	0 μg/mL	29	4.5	6.4
	6	0.03 μg/mL	28	3.5	8.0
	6	0.1 μg/mL	8.7	24	0.36
	6	0.3 μg/mL	3.8	35	0.11
	6	3.0 μg/mL	5.5	39	0.14
	6 + verapamil	3.0 μg/mL	15	21	0.71
V	none	0 ng/mL	30	4.5	6.7
	7	10 ng/mL	30	7.1	4.2
	7	30 ng/mL	24	11	2.2
	7	100 ng/mL	6.7	23	0.29

[a] At the start of each experiment, medium was changed to DMEM without phenol red or serum, with additions as indicated. After 45 min (experiments I, II, IV, and IV), or 30 min (experiment III), at 37 °C in CO_2/air, cells were processed for analysis. Values shown are 10^8 × mol of K^+ or Na^+ per dish, assayed as described previously.[13] When present, quinine was at 150 μM, verapamil at 100 μM.

Ion Transport and Estrogen Receptor Binding Activity of Bisphenols 4 and 5 and Related Compounds. The synthetic bisphenol derivatives **4** and **5** were tested by measuring changes in K^+ and Na^+ in HF cells. The fluorene derivative **5** was active at quite low concentrations and produced 50% of the maximum effect between 30 and 60 ng/mL (80−160 nM) (Table 2).

The bisphenol xanthene derivative **4** displayed partial activity in the assay for cell K^+ and Na^+ content. The

Scheme 3. Mechanisms by which Phenol Red (**1**) and Compounds **4** and **5** Might Be Formed

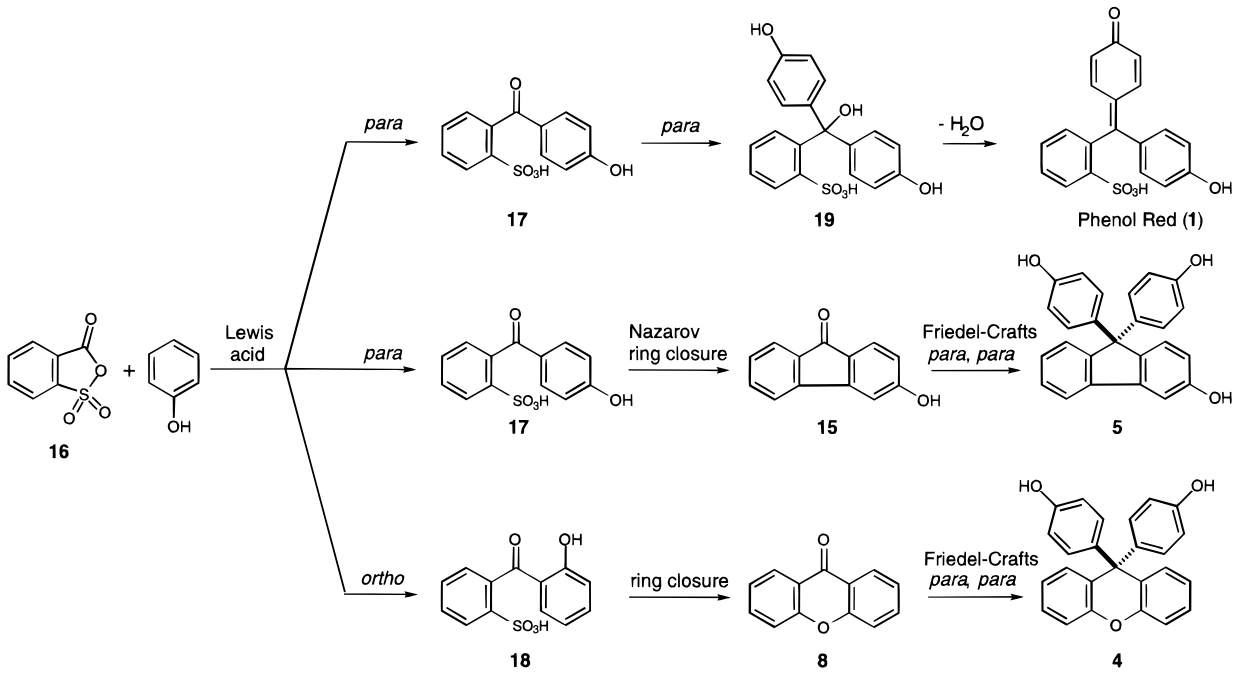

concentration that produced 50% of the maximum effect was between 2 and 5 μg/mL (5.5−14 μM). This compound is more interesting, however, because of its cytotoxicity. At concentrations not much greater than that which reduced cell K^+ by about 50% of control values, the bisphenol xanthene **4** caused cells to be released from the plastic substrate. This effect on cell adhesion made it impossible to obtain satisfactory dose−response data for **4**, as the affected cells were washed away during processing of the dishes (data not shown). Compound **6** was active in the bioassay at 0.1 μg/mL (280 nM) and **7** at 30 ng/mL (80 nM).

As described in previous reports on crude phenol red,[13,14] quinine and verapamil partially inhibit the action of **5** and **4** on ion content of human fibroblasts. Verapamil also partially inhibited the action of both **6** and **7** on cell K^+ and Na^+ (Table 2 and data not shown). Neither compound caused cells to detach from the plastic substrate. Hence, we think it likely that compounds **5**−**7**, and possibly **4**, all act on ion channels. Both quinine and verapamil have been well studied by others: These agents inhibit the activity of several types of ion channels, including K^+ and Ca^{2+} channels.[18,19]

We have also tested bisphenols **4**−**7** for their competitive binding affinities for the estrogen receptor (ER).[20] We found them to exhibit weak, competitive binding for the ER; the highest affinity compound, bisphenol **4**, had a relative binding affinity[20] (RBA) of 0.03% (where estradiol is 100%). The relative binding affinities of bisphenols **5**−**7** are 0.006%, 0.007%, and 0.010%, respectively. The RBA of phenol red prior to extraction is 0.010%, and the RBA of the crude ether extract of phenol red is 0.160%. The increased RBA value for the crude ether extract reflects the presence of the high-affinity bisphenol sulfonate **2** (50% relative to estradiol) which has previously been identified as a lipophilic impurity in phenol red.[9] Compound **2** showed no significant effect on cell K^+ and Na^+ content, when tested on MCF-7 cells at 15 μg/mL (35 μM) (data not shown).

Putative Mechanism of Formation of Bisphenols 4 and 5 During the Synthesis of Phenol Red. It is intriguing to speculate on the mechanism of formation of bisphenols **4** and **5** during the synthesis of phenol red. At the elevated temperatures required to effect the Friedel−Crafts reaction between phenol and 2-sulfobenzoic acid cyclic anhydride (**16**), the alkylation can occur at either the *para* (major) or the *ortho* (minor) positions of phenol (Scheme 3). Bisalkylation at the *para* position followed by subsequent elimination of water results in formation of phenol red (**1**) as the major product. Formation of 3-hydroxyfluorenone **15**, the precursor to bisphenol **5**, might be occurring from sulfonic acid **17** by electrocyclic Nazarov ring closure,[21] driven by the ultimate elimination of the sulfonic acid as sulfur dioxide and water from the initial cyclization product. Nazarov rearrangements are not precedented in the fluorenone system.[21] Nevertheless, a Nazarov-like electrocyclic ring closure might occur from a bisphenol species formed by the reaction of **17** with phenol.

The xanthone (**8**) precursor to **4** could be formed in a similar manner from **16** by initial attack of phenol at the *ortho* position to provide **18** (Scheme 3). Hydroxyl attack at the sulfonic acid-substituted aromatic carbon, followed by elimination of sulfonic acid as sulfur dioxide and water, would form xanthone (**8**). Ring closure could also occur after a molecule of phenol has added to **18**, as was discussed as an alternate mechanism for formation of the fluorene ring system (*vide supra*).

Conclusion

Two bisphenol derivatives with biological activity have been isolated from the lipophilic impurities present in a commercial preparation of phenol red; their structures have been determined by corroboration of ^1H and ^{13}C NMR methods and mass spectrometry and confirmed by synthesis. The bisphenol fluorene derivative **5** has been found to exhibit a rapid effect on the intracellular content of K^+ and Na^+ ions in human fibroblasts. The concentration that produces 50% of the maximum loss of K^+ and gain of Na^+ lies between 30 and 60 ng/mL (80−160 nM). The 2- and 4-hydroxy isomers of the fluorene compound, compounds **6** and **7**, prepared by synthesis are also active, 0.1 μg/mL (280

nM) and 30 ng/mL (80 nM), respectively. The bisphenol xanthene derivative **4** elicits a similar biological response but is less potent, and it also exhibits a marked effect on cell adhesion, causing release of cells from the plastic substrate at concentrations as low as 2 μg/mL.

The bisphenols would be expected to have their full effect when cells are in protein-free media, causing a fall in the steep gradients of monovalent ions that normally exist across the plasma membrane. These gradients, with intracellular K^+ often about 20 times higher than extracellular K, and with the reverse for Na, are necessary for cell function.[24] When cell K^+ decreases, intracellular processes that depend on K^+ may be compromised. The list of K-dependent processes is long and includes protein synthesis, as has been known for a long time, the recently reported stabilization of chaperone-ADP binding, and suppression of interleukin-1β maturation.[25−30]

The effect of these bisphenols on ion gradients could be masked in part if the Na^+/K^+ ATPase (the Na^+ pump), which continually removes excess intracellular Na, were active. Since they do deplete cells of K, even in the presence of an active Na^+ pump, the increase in the rates of K^+ efflux and Na^+ influx must be substantial. In fact, as Hopp et al. have shown, even though Na^+ pump activity is enhanced by phenol red impurities, it fails to prevent a sharp fall in K^+ and Na^+ gradients.[14]

The bisphenols are therefore quite efficacious. Potency, with an EC_{50} as low as 80−160 nM, is comparable to the potency of other inhibitors known to cause K^+ and Na^+ gradients to drop. The EC_{50} for ouabain, for example, an inhibitor of the Na^+ pump, is 20−30 nM in human cells.[31] The EC_{50} for amphotericin B, in mouse sarcoma-180 cells, is about 2 μM.[26] The calcium ionophore ionomycin, with an EC_{50} about 1 μM in EJ human bladder carcinoma cells, also causes marked loss of cell K.[13] The agent of ciguatera poisoning, maitotoxin, produced by a marine dinoflagellate, is extraordinarily potent; in addition to activating calcium influx, maitotoxin causes collapse of K^+ and Na^+ gradients in mouse BC_3H_1 cells at only 3 nM.[32]

Because verapamil and quinine partly inhibit the effect of the bisphenols, they presumably interact with ion channels. The full explanation of how the bisphenols act, however, will require studies by patch-clamp methods.

Experimental Section

General. Reaction progress was monitored by analytical thin-layer chromatography, using 0.25 mm silica gel glass-backed plates with F-254 indicator (Merck). Flash chromatography was performed with Woelm 32−63 μm silica gel packing.[22] Visualization was accomplished by phosphomolybdic acid or UV illumination (254, 350 μM). Reversed-phase HPLC was performed on a preparative Partisil M9 10 mm × 50 cm ODS-2 column or an analytical MicroPak 4 mm × 30 cm C-18 silica gel column. Phenol red monosodium salt (Lot #01601LF) was purchased from Aldrich Chemical Co. (Milwaukee, WI). Full spectroscopic characterization of compounds **4**−**7**, **18**, and **19** is given in the Supporting Information.

Chemical Syntheses. 9,9-Bis(4′-hydroxyphenyl)xanthene (4). To a solution of xanthone (**8**) (2.39 g, 12.2 mmol) stirring neat in phenol (22.8 g, 242.4 mmol) at 60 °C was added aluminum chloride (4.88 g, 36.6 mmol). The reaction mixture was heated to 180 °C and stirred for 12 h. The reaction mixture was allowed to cool to 80 °C, and excess phenol was removed *in vacuo*. Flash chromatography (silica gel, 4:1 hexanes:EtOAc to 2:1 hexanes:EtOAc) afforded the bis-*para*-substituted bisphenol **4** (1.37 g, 30%) as a white solid (mp 230−231 °C, lit.[16] mp 241 °C). Anal. ($C_{25}H_{18}O_3$) C, H.

9,9-Bis(4′-hydroxyphenyl)-3-hydroxyfluorene (5). Method A: To a solution of 1-hydroxyfluorenone (**11**) (0.115 g, 0.586 mmol) stirring neat in phenol (3.0 g, 31.8 mmol) at 60 °C was added aluminum chloride (0.234 g, 1.76 mmol). The reaction mixture was heated to 160 °C and stirred for 4 h. The reaction mixture was allowed to cool to 80 °C, and excess phenol was removed *in vacuo*. Flash chromatography (silica gel, 4:1 hexanes:EtOAc to 2:1 hexanes:EtOAc) afforded the bis-*para*-substituted bisphenol **5** (0.205 g, 35%) as the major product. Reversed-phase HPLC (50% H_2O, 50% CH_3CN) afforded **5** as a white solid.

Method B: To a solution of 3-hydroxyfluorenone (**19**) (0.089 g, 0.45 mmol) stirring neat in phenol (1.30 g, 13.8 mmol) at 60 °C was added aluminum chloride (0.191 g, 1.43 mmol). The reaction mixture was heated to 80 °C and allowed to stir for 2 h. Flash chromatography (4:1 hexanes:EtOAc to 2:1 hexanes:EtOAc) afforded bisphenol **5** (0.133 g, 81%) as the major product. Recrystallization in ether−hexanes gave **5** as a white crystalline solid (mp 248−250 °C). HRMS (EI) calcd for $C_{25}H_{18}O_3$ 366.1256, found 366.1254.

9,9-Bis(4′-hydroxyphenyl)-2-hydroxyfluorene (6). To a solution of 2-hydroxyfluorenone (**9**) (0.202 g, 1.03 mmol) stirring neat in phenol (3.0 g, 31.8 mmol) at 60 °C was added aluminum chloride (0.442 g, 3.09 mmol). The reaction mixture was heated to 80 °C, stirred for 2 h, and allowed to cool to room temperature. Flash chromatography (silica gel, 4:1 hexanes:EtOAc to 2:1 hexanes:EtOAc) afforded **6** (0.339 g, 89%) as a white solid (mp 264−266 °C). HRMS (EI) calcd for $C_{25}H_{18}O_3$ 366.1256, found 366.1262.

9,9-Bis(4′-hydroxyphenyl)-4-hydroxyfluorene (7). To a solution of 4-hydroxyfluorenone (**10**) (0.090 g, 0.46 mmol) stirring neat in phenol (1.29 g, 13.7 mmol) at 60 °C was added aluminum chloride (0.183 g, 1.37 mmol). The reaction mixture was heated to 80 °C, stirred for 2 h, and allowed to cool to room temperature. Flash chromatography (silica gel, 4:1 hexanes:EtOAc to 2:1 hexanes:EtOAc) afforded **7** (85%) as a white solid (mp 261−263 °C). Anal. ($C_{25}H_{18}O_3$) C, H.

Ethyl 2-(3′-Methoxyphenyl)benzoate (14). Ethyl 2-bromobenzoate (**12**) (2.50 g, 10.9 mmol) and tetrakistriphenylphosphinepalladium (0.43 g, 0.32 mmol) were dissolved in 115 mL of 1,2-dimethoxyethane. A 2 M aqueous solution of Na_2CO_3 (10.9 mL) was added *via* syringe. A solution of the boronic acid **13** (1.84 g, 12.0 mmol) in 10 mL of DME was subsequently added. The reaction mixture was heated to 100 °C and allowed to stir for 12 h. It was then cooled, diluted with water, extracted with ethyl acetate, and washed with saturated aqueous $NaHCO_3$ and brine. The organic layer was dried over $MgSO_4$, and the solvent was evaporated under reduced pressure to give a brown oil. Flash chromatography (8:1 hexanes:EtOAc to 1:1 hexanes:EtOAc) afforded 1.06 g (38%) of the biaryl compound **14** as a colorless oil. Anal. ($C_{16}H_{16}O_3$) C, H.

3-Hydroxy-9-fluorenone (15). A solution of biaryl compound **14** (0.756 g, 2.95 mmol) in 40 mL of methanesulfonic acid (59.2 g, 616 mmol) was stirred and heated to 110 °C for 1 h. The resulting black mixture was poured slowly into stirred ice water and then extracted with two portions of diethyl ether. The combined organic layers were washed with saturated $NaHCO_3$ solution and water and then dried over $MgSO_4$. The solvent was evaporated under reduced pressure to give a brown oil. Flash chromatography (8:1 hexanes:EtOAc) yielded 0.378 g (61%) of the desired 3-methoxy-9-fluorenone**.** To a solution of 3-methoxy-9-fluorenone (0.20 g, 0.94 mmol) in 10 mL of CH_2Cl_2 at 0 °C was added the boron trifluoride−dimethyl sufide complex (4.9 mL, 47 mmol). Upon addition of the complex, the reaction mixture turned from yellow to dark red in color. It was allowed to warm to room temperature and stir for 48 h. The reaction mixture was then added to water and extracted with three portions of ethyl acetate. The combined organic layers were dried over $MgSO_4$, and the solvent was evaporated under reduced pressure to a brown solid. Flash chromatography (10:1 hexanes:EtOAc to 2:1 hexanes:EtOAc) yielded 0.067 g (37%) of the yellow solid **15** (mp 227−228 °C, lit.[23] mp 228−229 °C). HRMS (EI) calcd for $C_{13}H_8O_2$ 196.0524, found 196.0521.

Bioassay. Human foreskin fibroblasts (HF) were grown in 6 cm diameter plastic tissue culture dishes in Dulbecco's modified Eagle's medium (DMEM) (GIBCO/Life Technologies, Grand Island, NY) with penicillin, streptomycin, neomycin, and 10% fetal bovine serum (HyClone Laboratories, Logan, UT) at 37 °C in CO_2/air, pH 7.2−7.4. For all experiments, DMEM without phenol red (Sigma Chemical, St. Louis, MO) was freshly prepared from powder. Quinine and verapamil were from Sigma. Stocks of dried HPLC fractions or of compounds **4**−**7**, prepared by synthesis, were dissolved in either dimethyl sulfoxide or ethanol. Solvents in test solutions were at 0.2% or less and had no activity.

For each experiment, values given in Tables 1 and 2 were averaged from duplicate dishes; duplicates usually differed by no more than 10−15%. Cell numbers per dish were from 5×10^5 to 2×10^6. Medium was replaced with test solution by four rapid rinses, with a final addition of 2.5 mL to each dish. After incubation as described in Tables 1 and 2, each dish was rapidly rinsed six times with iced 0.1 M $MgCl_2$ or 0.15 $MgSO_4$, and the excess was removed by suction. After the dishes were dry, 1.5 mL of the flame photometer diluent, lithium nitrate, was added; three freeze−thaw cycles followed, and the diluent, now containing the K^+ and Na^+ extracted from cells, was analyzed in a flame photometer.[24]

Acknowledgment. We are grateful for support of this research through a grant from the National Institutes of Health (PHS 5R37 DK15556 (J.A.K.)). We thank Kathryn E. Carlson for estrogen receptor binding affinity measurements.

Supporting Information Available: Full spectroscopic information on compounds **4**−**7**, **14**, and **15**, 1D and 2D ^1H and ^{13}C NMR spectra on compounds **4**−**6** and **19**, and HPLC traces on compounds **5** and **6** (14 pages). See any current masthead page for ordering information.

References

(1) Rowntree, L. G.; Geraghty, J. T. An Experimental and Clinical Study of the Functional Activity of the Kidneys by means of Phenosulphonephthalein. *J. Pharmacol. Exp. Ther.* **1910**, *1*, 579−661.

(2) Relman, A. S.; Levinsky, N. G. Clinical Examination of Renal Function. In *Diseases of the Kidney*; Strauss, M. B., Welt, L. G., Eds.; Little, Brown: Boston, 1971; pp 87−137.

(3) Maslen, C.; Stevens, T. R.; Hall, N. D. The Generation of Lipid Peroxides by Stimulated Human Neutrophils. Detection Using Phenol Red Oxidation. *J. Immunol. Methods* **1987**, *98*, 71−76.

(4) Orndorff, W. R.; Sherwood, F. W. Phenolsulfonephthalein and Some of Its Derivatives. *J. Am. Chem. Soc.* **1923**, *45*, 486−500.

(5) (a) Berthois, Y.; Katzenellenbogen, J. A.; Katzenellenbogen, B. S. Phenol Red in Tissue Culture Media is a Weak Estrogen: Implication Concerning the Study of Estrogen-Responsive Cells in Culture. *Proc. Natl. Acad. Sci. U.S.A.* **1986**, *83*, 2496−2500. (b) Katzenellenbogen, B. S.; Kendra, K. L.; Norman, M. J.; Berthois, Y. Proliferation, Hormonal Responsiveness, and Estrogen Receptor Content of MCF-7 Human Breast Cancer Cells Grown in the short-Term and Long-Term Absence of Estrogens. *Cancer Res.* **1987**, *47*, 4355−4360.

(6) Welshons, W. V.; Wolf, M. F.; Murphy, C. S.; Jordan, V. C. Estrogenic Activity of Phenol Red. *Mol. Cell. Endocrinol.* **1988**, *57*, 169−178.

(7) Glover, J. F.; Irwin, J. T.; Darbre, P. D. Interaction of Phenol Red with Estrogenic and Antiestrogenic Action on Growth of Human Breast Cancer Cells ZR-75-1 and T-47-D. *Cancer Res.* **1988**, *48*, 3693−3697.

(8) Bindal, R. D.; Carlson, K. E.; Katzenellenbogen, B. S.; Katzenellenbogen, J. A. Lipophilic Impurities, not Phenolsulfonphthalein, Account for the Estrogenic Activity in Commercial Preparations of Phenol Red. *J. Steriod Biochem.* **1988**, *31*, 287−293.

(9) Bindal, R. D.; Katzenellenbogen, J. A. Bis(4-hydroxyphenyl)-[2-(phenoxysulfonyl)-phenyl]methane: Isolation and Structure Elucidation of a Novel Estrogen from Commercial Preparations of Phenol Red (Phenolsulfonphthalein). *J. Med. Chem.* **1988**, *31*, 1978−1983.

(10) Grady, L. H.; Nonneman, D. J.; Rottinghaus, G. E.; Welshons, W. V. pH-Dependent Cytotoxicity of Contaminants of Phenol Red for MCF-7 Breast Cancer Cells. *Endocrinology* **1991**, *129*, 3321−3330.

(11) Greenberg, S. S.; Johns, A.; Kleha, J.; Xie, J.; Wang, Y.; Bianchi, J.; Conley, K. Phenol Red is a Thromboxane A_2/Prostaglandin H_2 Receptor Antagonist in Canine Lingual Arteries and Human Platelets. *J. Pharmacol. Exp. Ther.* **1994**, *268*, 1352−1361.

(12) Walsh-Reitz, M. M.; Toback, F. G. Phenol Red Inhibits Growth of Renal Epithelial Cells. *Am. J. Physiol.* **1992**, *262* (*Renal Fluid Electrolyte Physiol. 31*), F687−F691.

(13) Lubin, M. An Impurity in Phenol Red Opens an Ion Channel in Cultured Human Cells. *In Vitro Cell. Dev. Biol.* **1993**, *29A*, 597−600.

(14) (a) Hopp, L.; Bunker, C. H. Lipophilic Impurity of Phenol Red is a Potent Cation Transport Modulator. *J. Cell. Physiol.* **1993**, *157*, 594−602. (b) Hopp, L.; Bunker, C. H.; Day, B. W. Quinine Sensitive Changes in Cellular Na^+ and K^+ Homeostasis of COS-7 Cells Caused by a Lipophilic Phenol Red Impurity. *In Vitro Cell. Dev. Biol.* **1995**, *31*, 352−360.

(15) (a) Pretsch, E.; Seibl, J.; Simon, W.; Clerc, T. Effect of Substituents on the ^{13}C-Chemical Shifts in Monosubstituted Benzenes. In *Tables of Spectral Data for Structure Determination of Organic Compounds*; Boschke, F. L., Fresenius, W., Huber, J. F. K., Pungor, E., Rechnitz, G. A., Simon, W., West, T. S., Eds.; Springer-Verlag: Berlin, 1989; pp C120, C125. (b) Levy, G. C.; Lichter, R. L.; Nelson, G. L. *Carbon-13 Nuclear Magnetic Resonance Spectroscopy*; Wiley-Interscience: New York, 1980; p 110.

(16) Morgan, P. W. Aromatic Polyesters with Large Cross-Planar Substituents. *Macromolecules* **1970**, *3* (5), 536−544.

(17) (a) Miyaura, N.; Yanagi, T.; Suzuki, A. The Palladium-Catalyzed Cross-Coupling Reaction of Phenylboronic Acid with Haloarenes in the Presence of Bases. *Synth. Commun.* **1981**, *11*, 513−519. (b) Brown, A. G.; Crimmin, M. J.; Edwards, P. D. Application of the Suzuki Biphenyl Synthesis to the Natural Products Biphenomycin and Vancomycin. *J. Chem Soc., Perkin Trans. 1* **1992**, 123−130.

(18) (a) Weaver, J. L.; Szabo, G.; Pine, P. S.; Gottesman, M. M.; Goldenberg, S.; Aszalos, A. The Effect of Ion Channel Blockers, Immunosuppressive Agents, and Other Drugs on the Activity of the Multi-Drug Transporter. *Int. J. Cancer* **1993**, *54* (3), 456−461. (b) Amigorena, S.; Choquet, D.; Teillaud, J. L.; Korn, H.; Fridman, W. H. Ion Channel Blockers Inhibit B Cell Activation at a Precise Stage of the G1 Phase of the Cell Cycle. *J. Immunol.* **1990**, *144* (6), 2038−2045.

(19) (a) Munro, E.; Patel, M.; Chan, P.; Betteridge, L.; Gallagher, K.; Schachter, M.; Wolfe, J.; Sever, P. Effect of Calcium Channel Blockers on the Growth of Human Vascular Smooth Muscle Cells Derived from Saphenous Vein and Vascular Graft Stenoses. *J. Cardiovasc. Pharmacol.* **1994**, *23* (5), 779−784. (b) Rampe, D.; Wible, B.; Fedida, D.; Dage, R. C.; Brown, A. M. Verapamil Blocks a Rapidly Activating Delayed Rectifier K^+ Channel Cloned from Human Heart. *Mol. Pharmacol.* **1993**, *44* (3), 642−648.

(20) Katzenellenbogen, J. A.; Johnson, H. J.; Carlson, K. E. Studies on the Uterine, Cytoplasmic Estrogen Binding Protein. Thermal Stability and Ligand Dissociation Rate. An Assay of Empty and Filled Sites by Exchange. *Biochemistry* **1973**, *12*, 4092−4099.

(21) Reviewed in: (a) Santelli-Rouvier, C.; Santelli, M. The Nazarov Cyclization. *Synthesis* **1983**, *6*, 429−442. (b) Krohn, K. Nazarov and Pauson-Khand Reactions. *Organic Synthesis Highlights*; VCH: Weinheim, 1991; pp 137−144.

(22) Still, W. C.; Kahn, M.; Mitra, A. Rapid Chromatographic Technique for Preparative Separations with Moderate Resolution. *J. Org. Chem.* **1978**, *43*, 2923−2925.

(23) Ullmann, F.; Bleier, H. Zur Darstelluag von *o*-Aminobenzophenonderivaten. *Ber. Dtsch. Chem. Ges.* **1902**, *35*, 4273−4280.

(24) Lubin, M. K^+ Efflux in NIH Mouse 3T3 Cells and Transformed Derivatives: Dependence on Extracellular Ca^{2+} and Phorbol Esters. *Proc. Natl. Acad. Sci. U.S.A.* **1988**, *85*, 5097−5101.

(25) Lubin, M. Intracellular Potassium and Control of Protein Synthesis. *Fed. Proc.* **1964**, *23*, 994−1001.

(26) Lubin, M. Intracellular Potassium and Macromolecular Synthesis in Mammalian Cells. *Nature (London)* **1967**, *213*, 451−453.

(27) Kernan, R. P. *Cell Potassium*; Wiley-Interscience: New York, 1980.

(28) Lubin, M. Cell Potassium and the Regulation of Protein Synthesis. In *The Cellular Functions of Membrane Transport;* Hoffman, J. F., Ed.; Prentice-Hall: Englewood Cliffs, NJ, 1964; pp 193−211.

(29) Feifel, B.; Sandmeier, E.; Schonfeld, H.-J.; Christen, P. Potassium Ions and the Molecular-Chaperone Activity of DnaK. *Eur. J. Biochem.* **1996**, *237*, 318−321.

(30) Walev, I.; Reske, K.; Palmer, M.; Valeva, A.; Bhakdi, S. Potassium-inhibited processing of IL-1β in human monocytes. *EMBO J.* **1995**, *14*, 1607−1614.

(31) Ledbetter, M. L. S.; Lubin, M. Control of Protein Synthesis in Human Fibroblasts by Intracellular Potassium. *Exp. Cell Res.* **1977**, *105*, 223−236.

(32) Sladeczek, F.; Schmidt, B. H.; Alonso, R.; Vian, L.; Tep, A.; Yasumoto, T.; Cory, R. N.; Bockaert, J. New Insights into Maitotoxin Action. *Eur. J. Biochem.* **1988**, *174*, 663−670.

JM960300K